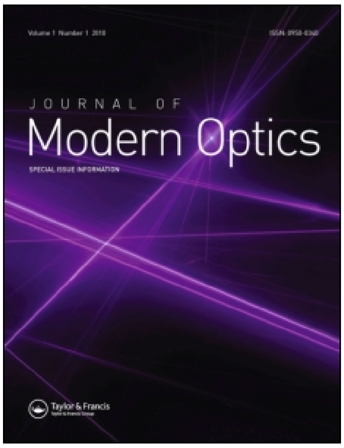

Journal of Modern Optics
Publication details, including instructions for authors and subscription information:
http://www.informaworld.com/smpp/title~content=t713191304

Polarisation singularities of non-paraxial Gaussian vortex beams diffracted by an annular aperture

Yongxin Liu[a,b]; Jixiong Pu[b]; Baida Lü[a]
[a] Institute of Laser Physics and Chemistry, Sichuan University, Chengdu, Sichuan 610064, China [b] College of Information Science & Engineering, Huaqiao University, Xiamen, Fujian 361021, China

First published on: 16 March 2011

To cite this Article Liu, Yongxin , Pu, Jixiong and Lü, Baida(2011) 'Polarisation singularities of non-paraxial Gaussian vortex beams diffracted by an annular aperture', Journal of Modern Optics, 58: 8, 657 — 664, First published on: 16 March 2011 (iFirst)

To link to this Article: DOI: 10.1080/09500340.2011.564319

URL: http://dx.doi.org/10.1080/09500340.2011.564319

Journal of Modern Optics
Vol. 58, No. 8, 10 May 2011, 657–664

Taylor & Francis
Taylor & Francis Group

Polarisation singularities of non-paraxial Gaussian vortex beams diffracted by an annular aperture

Yongxin Liu[a,b], Jixiong Pu[b]* and Baida Lü[a]

[a]*Institute of Laser Physics and Chemistry, Sichuan University, Chengdu, Sichuan 610064, China;*
[b]*College of Information Science & Engineering, Huaqiao University, Xiamen, Fujian 361021, China*

(*Received 25 January 2011; final version received 14 February 2011*)

Based on the vectorial Rayleigh–Sommerfeld diffraction integrals, the propagation expressions for non-paraxial Gaussian vortex beams diffracted by an annular aperture are derived, and are used to analyse polarisation singularities of non-paraxial Gaussian vortex beams in the diffraction field. It is shown that there exist polarisation singularities including C-points (S_{12} vortices), S_{23} vortices, and S_{31} vortices. The number and position of polarisation singularities depend on the waist width of the beam, the off-axis distance of the vortex and the aperture parameter. The creation and annihilation of polarisation singularities appear as a controlling parameter – including the waist width, off-axis distance and aperture parameter – varies. When compared with the free-space propagation, more polarisation singularities may take place in the diffraction field.

Keywords: polarisation singularities; non-paraxial; annular aperture; C-points

1. Introduction

Recently, singular optics has been extended not only from fully coherent wave fields (coherent singular optics) to partially coherent wave fields (correlation singular optics), but also from scalar wave fields to vector fields [1–14]. The method in experimental diagnostics of polarisation singularities by using a Mach–Zehnder interferometer was proposed by Oleg V. Angelsky et al. [14]. The polarisation singularities of strongly focused radially polarised beams was examined by Schoonover et al., where the different kinds of polarisation singularities including C-points, L-lines and V-points formed by radial and longitudinal electric-field components in the focal region were analysed [9].

The paraxial approximation is no longer valid when the beam width is comparable with the wavelength and/or the far-field divergence angle is large. It was shown that the polarisation singularities can be produced by means of the diffraction of Gaussian vortex beams beyond the paraxial approximation [13]. The purpose of the present paper is to study polarisation singularities of non-paraxial Gaussian vortex beams diffracted by an annular aperture, and to study the influence of the waist width of the beam, off-axis distance of the vortex and the aperture parameter on the number and the position of polarisation singularities.

2. Theoretical formulation

Consider a linearly polarised Gaussian vortex beam in the source plane $z=0$ whose electric field read as

$$E = E_x(x', y', 0)\vec{\mathrm{e}}_{\mathrm{x}}, \quad E_y(x', y', 0)\vec{\mathrm{e}}_{\mathrm{y}}, \tag{1}$$

where $\vec{\mathrm{e}}_{\mathrm{x}}$ and $\vec{\mathrm{e}}_{\mathrm{y}}$ are the unit vectors in the x and y directions,

$$E_x(x', y', 0) = \exp\left(-\frac{x'^2 + y'^2}{w_0^2}\right) \times [(x' - x_0) + i\,\mathrm{sgn}(l)(y' - y_0)]^{|l|}, \tag{2a}$$

$$E_y(x', y', 0) = 0, \tag{2b}$$

w_0 is the waist width of the Gaussian beam; x_0 and y_0 denote off-axis distances in the x and y directions, respectively; and l is the topological charge, we take $l=1$ in this paper; $\mathrm{sgn}(\cdot)$ is the sign function.

Assume that an annular aperture with inner radius a and outer radius b is placed in the plane $z=0$, whose window function is expressed as

$$T(x', y', 0) = \begin{cases} 1 & a^2 \le x'^2 + y'^2 \le b^2 \\ 0 & \text{otherwise} \end{cases} \tag{3}$$

In accordance with the vector Rayleigh-Sommerfeld diffraction integrals [15], the electric field

*Corresponding author. Email: jixiong@hqu.edu.cn

ISSN 0950–0340 print/ISSN 1362–3044 online

DOI: 10.1080/09500340.2011.564319
http://www.informaworld.com

of Gaussian vortex beams diffracted by the annular aperture in the z plane is expressed as

$$E_x(x,y,z) = -\frac{1}{2\pi}\int_{-\infty}^{\infty}\int_{-\infty}^{\infty} E_x(x',y',0)T(x',y',0) \times \frac{\partial G(\mathbf{r},\mathbf{r}')}{\partial z}\mathrm{d}x'\mathrm{d}y', \tag{4a}$$

$$E_y(x,y,z) = -\frac{1}{2\pi}\int_{-\infty}^{\infty}\int_{-\infty}^{\infty} E_y(x',y',0)T(x',y',0) \times \frac{\partial G(\mathbf{r},\mathbf{r}')}{\partial z}\mathrm{d}x'\mathrm{d}y', \tag{4b}$$

$$E_z(x,y,z) = \frac{1}{2\pi}\int_{-\infty}^{\infty}\int_{-\infty}^{\infty}\left[E_x(x',y',0)T(x',y',0)\frac{\partial G(\mathbf{r},\mathbf{r}')}{\partial x} + E_y(x',y',0)T(x',y',0)\frac{\partial G(\mathbf{r},\mathbf{r}')}{\partial y}\right]\mathrm{d}x'\mathrm{d}y', \tag{4c}$$

where $\mathbf{r}' = x'\vec{e}_x + y'\vec{e}_y$, $\mathbf{r} = x\vec{e}_x + y\vec{e}_y + z\vec{e}_z$, $\vec{e}_z$ is the unit vector in the z direction, and [16]

$$G(\mathbf{r},\mathbf{r}') = \frac{\exp(ik|r-r'|)}{|r-r'|}, \tag{5}$$

$$|r-r'| \approx r + \frac{x'^2 + y'^2 - 2xx' - 2yy'}{2r}, \tag{6}$$

with $k = 2\pi/\lambda$, $r' = \sqrt{x'^2 + y'^2}$, $r = \sqrt{x^2 + y^2 + z^2}$.

On substituting Equations (2), (3), (5) and (6) into Equations (4a)–(4c), and transforming Cartesian coordinates (x,y,z) into cylindrical coordinates (ρ,θ,z), and using the following formulas [17]

$$\int_0^{2\pi}\cos(n\theta)\exp[i\upsilon\cos(\theta)] = 2\pi i^n J_n(\upsilon), \tag{7}$$

$$J_n(\upsilon) = \sum_{m=0}^{\infty}\frac{(-1)^m}{m!(m+n)!}\left(\frac{\upsilon}{2}\right)^{2m+n}, \tag{8}$$

with $J_n(\cdot)$ being the nth Bessel function, after lengthy but direct integral calculations, we obtain

$$\begin{aligned}E_x(x,y,z) = &-\frac{ikz}{r^2}e^{ikr}(y-ix)\sum_{m=0}^{\infty}\frac{1}{m!(m+1)!} \times \frac{(x^2+y^2)^m}{2g^{m+2}}\left(\frac{k}{2r}\right)^{2m+1} \\ &\times\left[\Gamma(2+m,-a^2g)-\Gamma(2+m,-b^2g)\right] \\ &- q\sum_{m=0}^{\infty}\frac{1}{m!m!}\frac{(x^2+y^2)^m}{2g^{m+1}}\left(\frac{k}{2r}\right)^{2m} \\ &\times\left[\Gamma(1+m,-b^2g)-\Gamma(1+m,-a^2g)\right],\end{aligned} \tag{9a}$$

$$E_y(x,y,z) = 0, \tag{9b}$$

$$\begin{aligned}E_z(x,y,z) = \frac{ik}{r^2}e^{ikr}\Bigg\{ &-qx\sum_{m=0}^{\infty}\frac{(x^2+y^2)^m}{m!m!2g^{m+1}}\left(\frac{k}{2r}\right)^{2m} \\ &\times\left[\Gamma(1+m,-b^2g)-\Gamma(1+m,-a^2g)\right] \\ &-\sum_{m=0}^{\infty}\frac{(x^2+y^2)^m}{m!m!4g^{m+2}}\left(\frac{k}{2r}\right)^{2m} \\ &\times\left[\Gamma(2+m,-a^2g)-\Gamma(2+m,-b^2g)\right] \\ &+(xy-ix^2-ixq)\sum_{m=0}^{\infty}\frac{(x^2+y^2)^m}{m!(m+1)!2g^{m+2}} \\ &\times\left(\frac{k}{2r}\right)^{2m+1}\left[\Gamma(2+m,-a^2g)-\Gamma(2+m,-b^2g)\right] \\ &+(x^2-y^2+2ixy)\sum_{m=0}^{\infty}\frac{(x^2+y^2)^m}{m!(m+2)!4g^{m+3}}\left(\frac{k}{2r}\right)^{2m+2} \\ &\times\left[\Gamma(3+m,-b^2g)-\Gamma(3+m,-a^2g)\right]\Bigg\},\end{aligned} \tag{9c}$$

where $\Gamma(u,v)$ denotes the incomplete gamma function, and

$$g = \frac{ik}{2r} - \frac{1}{w_0^2}, \tag{10}$$

$$q = x_0 + iy_0. \tag{11}$$

Equations (9a)–(9c) are the analytical expressions for the non-paraxial Gaussian vortex beams diffracted by the annular aperture. Although Equations (9a) and (9c) contain the infinite series summation, the summation is convergent and in the numerical computation, we take the former 30 terms to approximate the infinite series summation, which fits quite well with the direct integration of Equations (4a)–(4c). Equations (9a)–(9c) are more general formulas, not only applicable to the annular aperture, but also to the circular aperture, circular screen and the free-space by letting $a \to 0$, $b \to \infty$, and $a \to 0$, $b \to \infty$, respectively. In addition, Equations (9a)–(9c) indicate that besides the transverse electric-field component $E_x(x,y,z)$, the longitudinal electric-field component $E_z(x,y,z)$ appears in the non-paraxial diffraction field.

In accordance with [9], the conversional description of the state of polarisation singularities formed by two transverse components can be used to describe the state of polarisation and polarisation singularities formed by transverse and longitudinal components in vector non-paraxial fields if the definition of the Stokes parameter is suitably changed, i.e.

$$s_0 = |E_z|^2 + |E_x|^2 \tag{12}$$

$$S_1 = s_0^{-1}(|E_z|^2 - |E_x|^2) \tag{13}$$

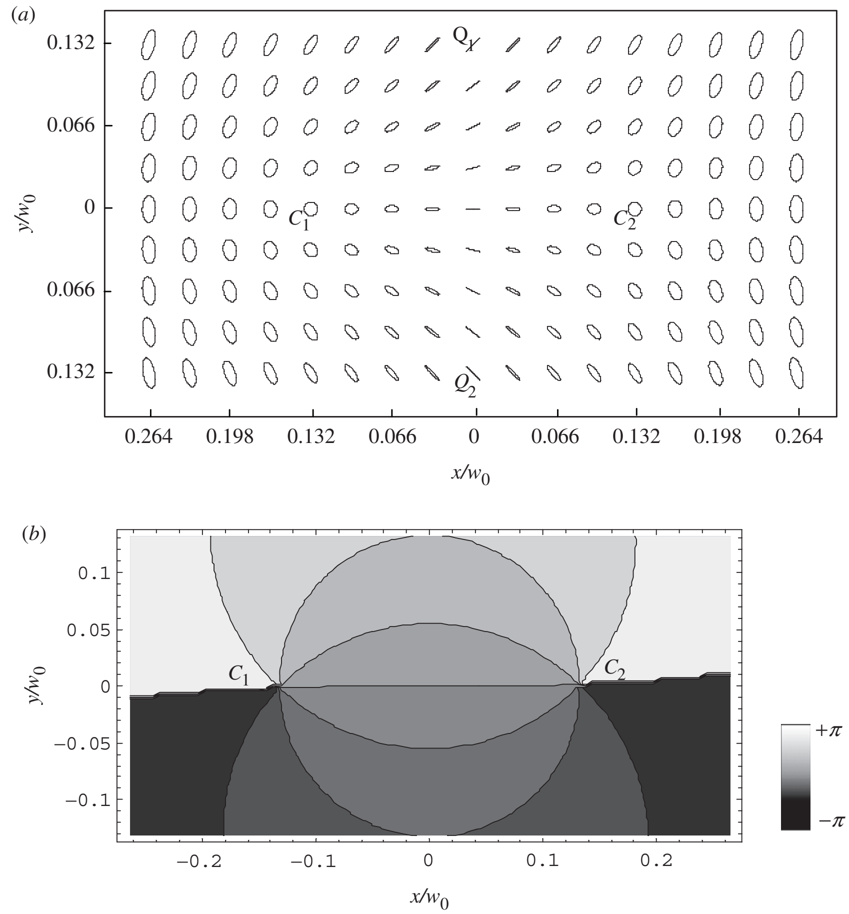

Figure 1. (*a*) The polarisation ellipses surrounding the C-points in the plane $z = 3z_r$ of a non-paraxial Gaussian vortex beam diffracted by an annular aperture. (*b*) The corresponding phase map of the complex Stokes field S_{12}. The calculation parameters are seen in the text.

$$S_2 = 2s_0^{-1}\mathrm{Re}(E_z^* E_x) \tag{14}$$

$$S_3 = 2s_0^{-1}\mathrm{Im}(E_z^* E_x) \tag{15}$$

where $S_1^2 + S_2^2 + S_3^2 = 1$. The contour lines of $S_1 = 0$, $S_2 = 0$, and $S_3 = 0$ can be marked by Z_1, Z_2, Z_3 lines, respectively. The Z_3 line is also called the *L*-line. The complex Stokes fields are given by [6]

$$S_{12} = S_1 + iS_2 \tag{16}$$

$$S_{23} = S_2 + iS_3 \tag{17}$$

$$S_{31} = S_3 + iS_1. \tag{18}$$

The S_{12} vortices (singularities) occur at the intersections of Z_1 and Z_2, i.e. $S_{12} = 0, |S_3| = 1$, which is also called the C-point. At the C-point, the polarisation ellipse reduces to a circle; thus the orientations of the major and minor axes of the polarisation ellipse are undetermined. $S_3 = +1$ (or –1) means right (or left) handedness, and C-points can be classified into monstar (singularity index $I_c = +\frac{1}{2}$), star ($I_c = -\frac{1}{2}$) and lemon ($I_c = +\frac{1}{2}$), respectively, based on the local behavior of the polarisation ellipse [14]. The S_{23} vortices appear at the intersections of Z_2 and Z_3, i.e. $S_{23} = 0, |S_1| = 1$. The S_{31} vortices are present as the intersections of Z_3 and Z_1, i.e. $S_{31} = 0, |S_2| = 1$. The S_{23} vortices and S_{31} vortices are on the contour lines of $S_3 = 0$ (i.e. L-lines), and for such a case the polarisation ellipse degenerates into a line, thus the handedness of the polarisation ellipse is undefined [6,7].

3. Numerical calculation results and analysis

Figure 1(*a*) gives the polarisation ellipses surrounding the C-points in the plane $z = 3z_r$ ($z_r = \frac{\pi w_0^2}{\lambda}$– Rayleigh range) of a non-paraxial Gaussian vortex beam diffracted by an annular aperture, and the calculation parameters are $w_0 = 1.2\,\lambda$, $x_0 = y_0 = 0$, $a = 0.8\,\lambda$, $\varepsilon = a/b = 0.3$. Figure 1(*b*) gives the corresponding

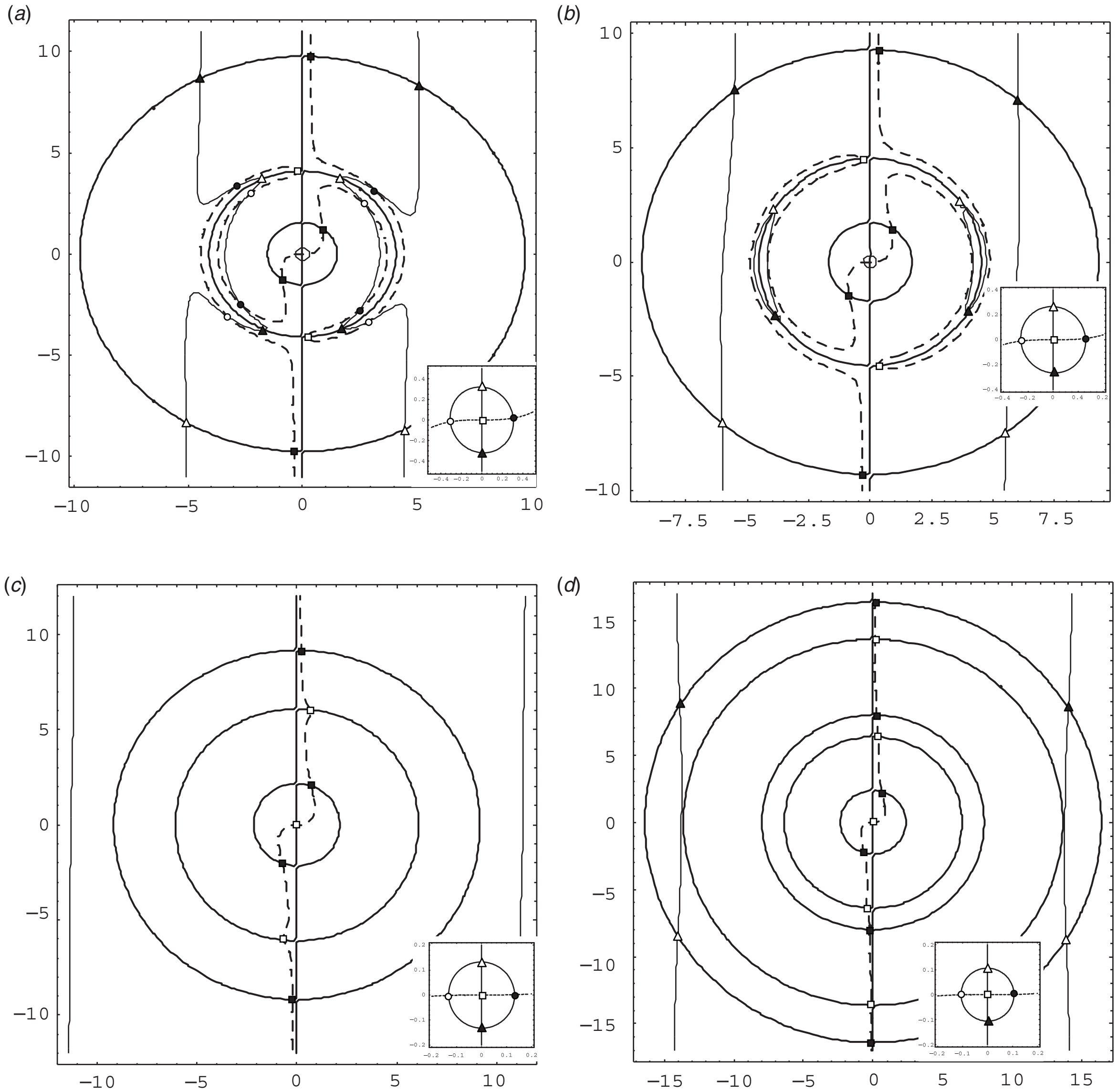

Figure 2. The contour lines Z_1, Z_2, Z_3 of non-paraxial diffracted Gaussian vortex beams in the $z=3z_r$ plane for different values of the waist width. (*a*) $w_0=0.5\,\lambda$, (*b*) $w_0=0.6\,\lambda$, (*c*) $w_0=1.2\,\lambda$, (*d*) $w_0=1.5\,\lambda$.

phase map of the complex Stokes field S_{12}. From Figure 1(*a*) we see there are two C-points C_1, C_2, and two S_{31} vortices Q_1, Q_2, which are on the L-line. When one pays attention to the surrounding polarisation ellipses of C_1 and C_2, there exist three straight-line trajectories of the direction of the major axis for both C_1 and C_2. From Figure 1(*b*) and according to the sign principle [19], we can get that the singularity index I_c of C_1 and C_2 points are $+\frac{1}{2}$, $-\frac{1}{2}$ corresponding to the topological charge +1, –1, respectively, and C_1 is a monstar, and C_2 is a star [18].

Figure 2 gives the contour lines Z_1, Z_2, Z_3 of non-paraxial diffracted Gaussian vortex beams in the $z=3z_r$ plane for different values of the waist width, which are marked by thin, dashed and thick curves, respectively. The calculation parameters are $x_0=y_0=0$, $a=0.8\,\lambda$, $\varepsilon=a/b=0.3$, and (*a*) $w_0=0.5\,\lambda$, (*b*) $w_0=0.6\,\lambda$, (*c*) $w_0=1.2\,\lambda$, (*d*) $w_0=1.5\,\lambda$. The S_{12} vortices (C-points), S_{23} vortices and S_{31} vortices are shown by circles, squares and triangles, and the black and white ones correspond to the topological charge $l=-1$ and $+1$, respectively. From Figure 2(*a*)–(*d*) we find that there exist S_{12} vortices (C-points), S_{23} vortices and S_{31} vortices in the diffraction field. By varying waist width from $0.5\,\lambda$ to $0.6\,\lambda$, four pairs of C-points with equal but opposite topological charge annihilate each other, which are C_3 and C_4, C_5 and C_6, C_7 and C_8, C_9 and C_{10}. Increasing w_0 to $1.2\,\lambda$, another four pairs

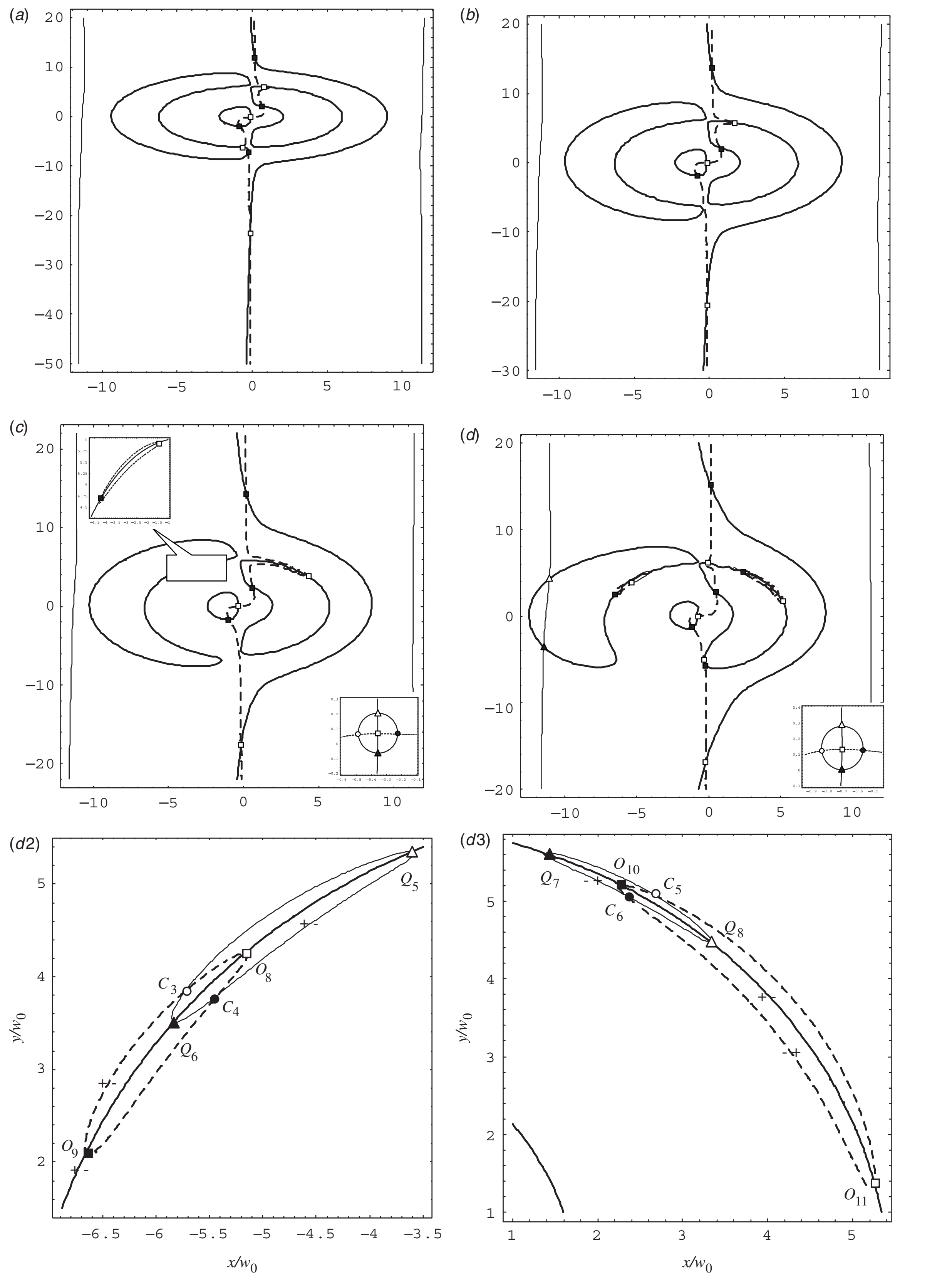

Figure 3. The contour lines Z_1, Z_2, Z_3 of non-paraxial diffracted Gaussian vortex beams in the $z = 3z_r$ plane for different values of the off-axis distance y_0. (*a*) $y_0 = 0.05\,\lambda$, (*b*) $y_0 = 0.1\,\lambda$, (*c*) $y_0 = 0.2\,\lambda$, (*d*1) $y_0 = 0.4\,\lambda$, (*d*2), (*d*3) are the partial enlarged figures for (*d*1).

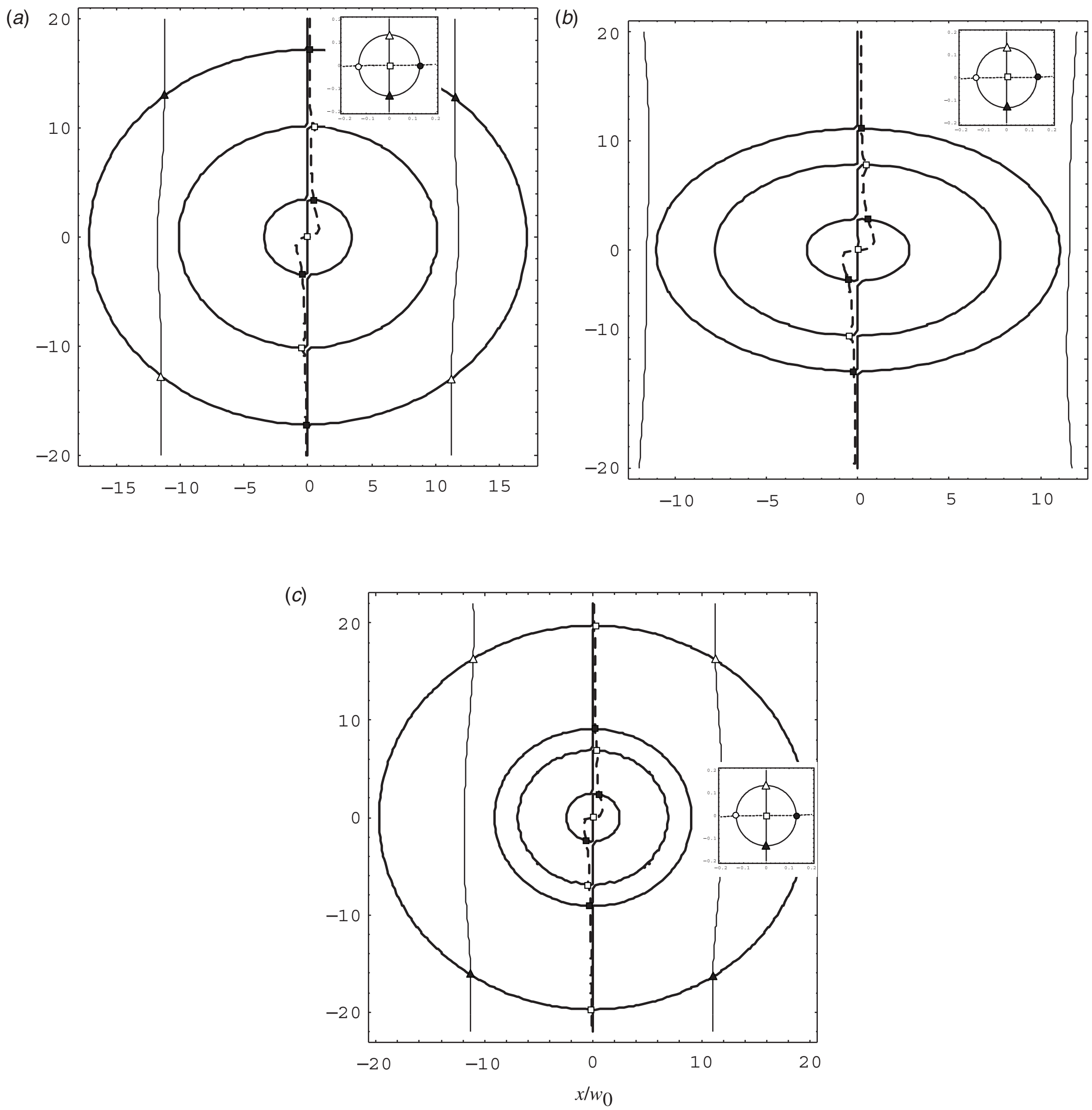

Figure 4. The contour lines Z_1, Z_2, Z_3 of a non-paraxial diffracted Gaussian vortex beam in the $z = 3z_r$ plane for different values of the inner radius a. (*a*) $a = 0.4\,\lambda$, (*b*) $a = 0.5\,\lambda$, (*c*) $a = 0.6\,\lambda$.

of S_{31} vortices with equal but opposite topological charge annihilate each other, which are Q_3–Q_{10}. Finally, with a further increment of w_0 to $1.5\,\lambda$, two pairs of S_{23} vortices (i.e. O_7–O_{10}) and two pairs of S_{31} vortices (i.e. Q_{11}–Q_{14}) occur in Figure 1(*d*). As can be seen, the creation and annihilation of polarisation singularities appear, but the handedness of C_1 and C_2 keeps unchanged as the waist width w_0 varies. C_1 is right-handed, while C_2 is left-handed.

Figure 3 plots the contour lines Z_1, Z_2, Z_3 of non-paraxial diffracted Gaussian vortex beams in the $z = 3z_r$ plane for different values of the off-axis distance y_0, where the calculation parameters are $a = 0.8\,\lambda$, $\varepsilon = a/b = 0.3$, $w_0 = 1.2\,\lambda$, $x_0 = 0$, and (*a*) $y_0 = 0.05\,\lambda$, (*b*) $y_0 = 0.1\,\lambda$, (*c*) $y_0 = 0.2\,\lambda$, (*d*1) $y_0 = 0.4\,\lambda$, (*d*2)–(*d*3) are the partial enlarged figure for (*d*1). It is seen from Figure 3(*a*)–(*c*) that a pair of S_{23} vortices O_3 and O_5 annihilate each other by increasing y_0 from $0.05\,\lambda$ to $0.1\,\lambda$, and a new pair of S_{23} vortices O_8 and O_9 appears as y_0 is increased to $0.2\,\lambda$. In Figure 3(*d*1)–(*d*3) for $y_0 = 0.4\,\lambda$, there exist six C-points, 12 S_{23} vortices and eight S_{31} vortices. In comparison with Figure 3(*c*), two pairs of C-points C_3–C_6, two pairs of S_{23} vortices O_{10}–O_{13} and three pairs of S_{31} vortices Q_3–Q_8 are the newly appeared polarisation singularities. In Figure 3(*d*2) and (*d*3) there exist a pair of

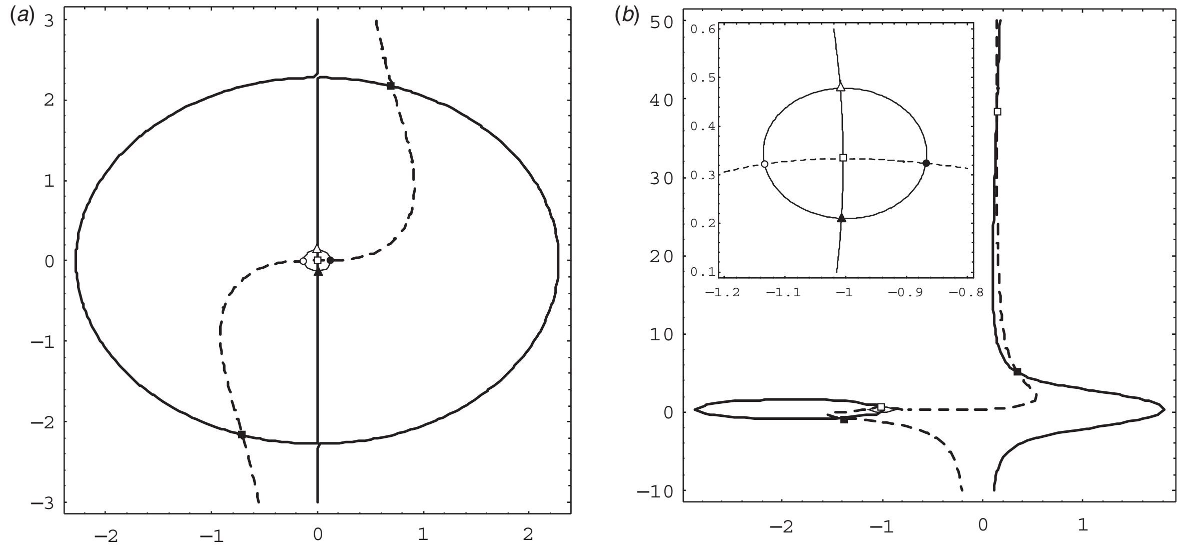

Figure 5. The contour lines Z_1, Z_2, Z_3 of non-paraxial Gaussian vortex beams in the $z=3z_r$ plane for different values of the off-axis distance. (*a*) $y_0=0$, (*b*) $y_0=0.4\,\lambda$.

C-points with equal but opposite topological charge, C_3–C_4 and C_5–C_6, respectively. C_3 and C_6 are right-handed, and C_4 and C_5 are left-handed. Therefore, the off-distance affects the number and position of polarisation singularities.

Figure 4 gives the contour lines Z_1, Z_2, Z_3 for a non-paraxial diffracted Gaussian vortex beam in the $z=3z_r$ plane for different values of the inner radius a of the annular aperture, where the calculation parameters are $w_0=1.2\,\lambda$, $x_0=y_0=0$, $\varepsilon=a/b=0.3$, and (*a*) $a=0.4\,\lambda$, (*b*) $a=0.5\,\lambda$, (*c*) $a=0.6\,\lambda$. It is found that the creation, motion and the annihilation of the polarisation singularities of the diffraction field appear as the inner radius of the annular aperture varies. In the variation of a from $0.4\,\lambda$ to $0.5\,\lambda$ in Figure 4(*a*)–(*b*), two pairs of S_{31} vortices (i.e. Q_3–Q_6) annihilate each other, and the S_{23} vortices O_1–O_6 move. For example, O_5 and O_6 move from ($-0.16\,w_0$, $-17.13\,w_0$), ($0.16\,w_0$, $17.13\,w_0$) to ($-0.19\,w_0$, $-11.06\,w_0$), ($0.19\,w_0$, $11.06\,w_0$), respectively. By increasing a to $0.6\,\lambda$, two pairs of S_{31} vortices (i.e. Q_7–Q_{10}) and two S_{23} vortices (i.e. O_7–O_8) appear in Figure 4(*c*). Further increasing a to $0.8\,\lambda$, the newly appeared L_7–L_{10} and O_7–O_8 annihilate each other, which can be seen from Figure 2(*c*). However, the handedness of C_1 and C_2 keeps unchanged in the variation of a, i.e. C_1 is right-handed, while C_2 is left-handed.

Figure 5 plots the contour lines Z_1, Z_2, Z_3 for non-paraxial Gaussian vortex beams in the $z=3z_r$ plane for different values of the off-axis distance, where the calculation parameters are $w_0=1.2\,\lambda$, $x_0=0$, $a\to 0$, $b\to\infty$, and (*a*) $y_0=0$, (*b*) $y_0=0.4\,\lambda$. As can be seen, when the off-axis distance y_0 is increased from zero to $0.4\,\lambda$, a new S_{23} vortex appear, which is labeled by O_4 in Figure 5(*b*). As compared with Figure 5(*b*) and Figure 3(*d*1), it is found that there exist two C-points, four S_{23} vortices and two S_{31} vortices in $z=3z_r$ in the free-space propagation (Figure 5(*b*)), while there are six C-points, 12 S_{23} vortices and eight S_{31} vortices in the diffraction field (Figure 3(*d*1)). Therefore, more polarisation singularities may appear in the diffraction field.

It can be shown that the topological relationship holds true for the polarisation singularities of non-paraxial Gaussian vortex beams diffracted by an annular aperture. The topological relationship between the topological charge of Stokes vortices is expressed as [6]

$$2\sigma_k \Sigma_{(k)} l_{ij} = \Sigma^{(K)}\sigma_i l_{jk} = \Sigma^{(k)}\sigma_j l_{ik} \tag{19}$$

where $\sum_{(k)}$ specifies summation over all the polarisation singularities contained within a closed contour line Z_k and $\sum^{(k)}$ denotes summation over the polarisation singularities on the Z_k, $\sigma_{i,j,k}=1$ for $S_{i,j,k}>0$ and $\sigma_{i,j,k}=-1$ for $S_{i,j,k}<0$, l_{ij} is the topological charge of the singularities. For example, we choose the closed contour line Z_2 in Figure 3(*d*2), the left term of Equation (19) is $2\sigma_2\sum_{(2)}l_{13}=2\times(-1)\times(-1)=2$, the middle one is $\sum^{(2)}\sigma_1 l_{32}=-1\times(-1)+1\times(+1)=2$, and the right one is $\sum^{(2)}\sigma_3 l_{12}=-1\times(-1)+1\times(+1)=2$.

4. Conclusion

In this paper, the propagation expressions for non-paraxial Gaussian vortex beams diffracted by an annular aperture have been derived, and used to analyse polarisation singularities of non-paraxial

Gaussian vortex beams in the diffraction field. It has been shown that there exist polarisation singularities including C-points (S_{12} vortices), S_{23} vortices, and S_{31} vortices, and C-points can be classified into stars, monstars and lemons. The number and position of polarisation singularities depend on the waist width, off-axis distance and aperture parameter. The creation and annihilation of polarisation singularities may appear as a controlling parameter including the waist width, off-axis distance and the aperture parameter varies. In comparison with the free-space propagation, more polarisation singularities may take place in the diffraction field.

Acknowledgements

This research was supported by the National Natural Science Foundation of China (Grant Nos. 10874125 and 60977068) and the Science Foundation of Huaqiao University (No. 10QZR03).

References

[1] Chernyshov, A.A.; Felde, Ch.V.; Bogatyryova, H.V.; Polyanskii, P.V.; Soskin, M.S. *J. Opt. A: Pure Appl. Opt.* **2009,** *11,* 094010.
[2] Soskin, M.S.; Polyanskii, P.V. *Proc. SPIE.* **2010,** *V. 7613,* 76130G-1.
[3] Gbur, G.; Visser, T.D. *Prog. Opt.*, **2010,** *55,* 284–341.
[4] Felde, Ch.V.; Chernyshov, A.A.; Bogatyryova, H.V.; Polyanskii, P.V.; Soskin, M.S. *JETP Lett.* **2008,** *88,* 418–422.
[5] Freund, I. *Opt. Lett.* **2001,** *26,* 1996–1998.
[6] Freund, I.; Mokhun, A.I.; Soskin, M.S.; Angelsky, O.V.; Mokhun, I.I. *Opt. Lett.* **2002,** *27,* 545–547.
[7] Mokhun, A.I.; Soskin, M.S.; Freund, I. *Opt. Lett.* **2002,** *27,* 995–997.
[8] Soskin, M.S.; Dladimir, V.; Freund, I. *Opt. Lett.* **2003,** *28,* 1475–1477.
[9] Schoonover, R.W.; Visser, T.D. *Opt. Express* **2006,** *14,* 5733–5745.
[10] Dennis, M.R. *Opt. Commun.* **2002,** *213,* 201–221.
[11] Korotkova, O.; Wolf, E. *Opt. Lett.* **2005,** *30,* 198–200.
[12] Yan, H.W.; Lü, B.D. *Opt. Lett.* **2009,** *34,* 1933–1935.
[13] Luo, Y.M.; Lü, B.D. *J. Opt. Soc. Am. A* **2009,** *26,* 1961–1966.
[14] Angelsky, O.V.; Mokhun, I.I.; Mokhun, A.I.; Soskin, M.S. *Phy. Rev. E* **2002,** *65,* 036602.
[15] Luneburg., R.K. *Mathematical Theory of Optics*; University of California Press: Berkeley, CA, 1966.
[16] Duan, K.; Lü, B. *Opt. Lett.* **2004,** *29,* 800–802.
[17] Bronshtein, I.N.; Semendyayev, K.A. *Handbook of Mathematics*; Verlag Harri Deutsch Press: Thun and Frankfurt, 1979.
[18] Nye, J.F. *Natural Focusing and the Fine Structure of Light*; IOP Publishing: Bristol, UK, 1999.
[19] Freund, I.; Shvartsman, N. *Phys. Rev. A* **1994,** *50,* 5164–5172.